Electrochemical Study on 4-(azulen-1-yl)-2,6-bis(2-furyl)- and 4-(azulen-1-yl)-2,6-bis(2-thienyl)-pyridines

ELEONORA-MIHAELA UNGUREANU[1]*, GEORGE-OCTAVIAN BUICA[2], ALEXANDRU C. RAZUS[3], LIVIU BIRZAN[3], RAMONA WEISZ [1], MAGDALENA-RODICA BUJDUVEANU[1]

[1]University Politehnica of Bucharest, Faculty of Applied Chemistry and Material Sciences, 1-7 Gh. Polizu, 011061, Bucharest, Romania

[2] Petroleum-Gas University of Ploiesti, Bucuresti 39, 100680, Ploiesti, Romania

[3] Romanian Academy, Organic Chemistry Center "C. D. Nenitzescu", 202B Spl. Independentei,060023, Bucharest, Romania

An electrochemical study of 4-(azulen-1-yl)-2,6-bis(2-furyl)- and 4-(azulen-1-yl)-2,6-bis(2-thienyl)-pyridines was performed in order to estimate the influence of electron releasing alkyl substituents on the electrochemical behaviour of these azulenes. The electrochemical parameters obtained by cyclic and differential pulse voltammetry have been correlated with ionization potentials and LUMO energies evaluated through computational methods for the above compounds containing azulene moiety substituted with alkyl functional groups.

Keywords: 4-(azulen-1-yl)-2,6-bis(2-furyl)-pyridines; 4-(azulen-1-yl)-2,6-bis(2-thienyl)-pyridines; Cyclic Voltammetry (CV), Differential Pulse Voltammetry (DPV), Computations

Azulenes are nonbenzenoid aromatic compounds with a special structure, having a five-membered ring connected to a seven-membered ring. This link between rings with opposite electronic densities (high, respectively low) induces a peculiar electrochemistry: they can be involved easier than benzenoid aromatic compounds both in oxidation and in reduction reactions. However, it is known that azulene is a better electron donor than acceptor. Such compounds containing azulene in the molecule present valuable properties as enhanced nonlinear optics coefficients [1] and electrochromic behaviour [2]. Using electrochemical procedures, the azulene derivatives could generate polymers that have similar properties to the reported azulene polymers, which have high electrical conductivity [3]. This feature makes them attractive as cathode active materials for rechargeable batteries [4]. In spite of these potentialities, there are few electrochemical studies devoted to azulenes, regarding e.g. the generation of the polyazulene films [5] or metal complexes starting from azulene derivatives [6,7].

Azulene structure peculiarity enables to evaluate the influence of substituents nature and position on the electrochemical properties (number and potentials of redox waves, etc.). The present study is a part of a large investigation of azulene derivatives through electrochemical methods which has been done in our group [8-11]. This paper is devoted to the electrochemical study of new azulenyl-pyridines substituted with two furane or thiophene rings in α-position of pyridine, namely 4-(azulen-1-yl)-2,6-bis(2-furyl)- and 4-(azulen-1-yl)-2,6-bis(2-thienyl)-pyridines.

Experimental part

Reagents, instrumentation and methods

Acetonitrile (Rathburn, HPLC grade) and tetra-*n*-butylammonium perchlorate (TBAP) from Fluka were used as received for solvent and supporting electrolyte, respectively. The investigated compounds were synthesized starting from their carbonyl derivatives by specific chemical reactions [12]. Structure and physical characteristics were confirmed by elemental and spectral (^{1}H NMR, ^{13}C NMR, GC–MS) analyses. Cyclic voltammetry (CV) and differential pulse voltammetry (DPV) experiments were conducted in a conventional three-electrode cell under argon atmosphere at 25°C using a PGSTAT 12 AUTOLAB potentiostat. The working electrode was a glassy carbon disk (3-mm diameter from CH Instruments) polished with 0.1μm diamond paste. The Ag/10mM $AgNO_3$ in CH_3CN + 0.1M TBAP system was used as reference electrode. All potentials were referred to the potential of ferrocene/ferricinium (Fc/Fc^+), which was 0.07V with our experimental conditions. CV experiments were usually performed at 0.1 V/s, and with different scan rates (0.1–1V/s), for investigation of scan rate influence. DPV curves were recorded at 10mV/s with a pulse height of 25mV and a step time of 0.2 s.

Computational methods

Calculations were performed with a MOPAC package and AM1 approach.

Results and discussions

The investigated compounds are represented in figure 1. The azulene moiety is either unsubstituted, as in compounds **1** and **2**, or substituted in the seven-membered ring with electron releasing alkyl groups like 4,6,8-trimethyl as in compounds **1t** and **2t,** or with 3,8-dimethyl-5-isopropyl (guaiazulene derivatives), as in compounds **1g** and **2g**.

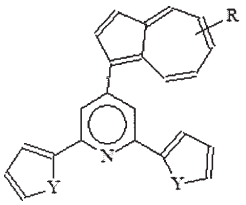

Y = O; R = H (**1**)
Y = O; R = 4,6,8-trimethyl (**1t**)
Y = O; R = 3,8-dimethyl-5-isopropyl (**1g**)
Y = S; R = H (**2**)
Y = S; R = 4,6,8-trimethyl (**2t**)
Y = S; R = 3,8-dimethyl-5-isopropyl (**2g**)

Fig. 1. Formula of the investigated compounds.

* *email: em_ungureanu2000@yahoo.com: Tel.: 0724659287*

For each compound, two complementary methods have been used in parallel for the electrochemical investigation: differential pulse voltammetry (DPV) and cyclic voltammetry (CV). Both DPV and CV studies have been accomplished in acetonitrile with 0.1M tetrabuthyl-ammonium perchlorate (TBAP) as supporting electrolyte in milimolar solutions of 4-(azulen-1-yl)-2,6-di(furyl)- or 2,6-di(tienyl)- pyridine. The evidenced peaks correspond to the oxidation and reduction processes which occur during scanning. For each compound, the DPV experiments at different concentrations enabled the precise evaluation of anodic and cathodic peak potentials and currents. The CV study was performed at different concentrations (0.5 – 3mM), scan rates and potential ranges in order to establish the reversibility/irreversibility of each process. The results obtained by CV and DPV were in agreement with respect to the peak potentials, and were complementary, yielding specific features for each process.

CV and DPV studies

Figures 2 and 3 show the characteristic DPV and CV curves obtained for the azulene derivative 1. Anodic and cathodic curves are shown together on each graph. When examining the DPV curve (fig .2) of the parent compound **1** in anodic scans, 3 peaks at 0.61V (1a), 0.89V (2a), and 1.076V (3a) can be observed, while in the cathodic scans, 3 reduction peaks are found at -1.76V (1c), -2.55V (2c), and -2.81V (3c). The DPV peak currents linearly increase with the concentration of **1**. The inset in figure 2 presents the variation of the peak currents with the concentration of compound **1**, as obtained from DPV experiments.

The processes 1a-3a and 1c-3c are also evidenced by CV. The cyclic voltammograms for the compound **1** at different concentrations are shown in Figure 3. Three anodic peaks at 0.617V (1a), 0.890V (2a), and 1.076V (3a), and 3 cathodic peaks at -1.76 V (1c), -2.55V (2c), and -2.81V (3c) can be observed. Each process from the cyclic voltammograms has been analyzed at different scan ranges with respect to the reversible character. Figure 4 shows that all the 3 oxidation processes of compound **1**, denoted 1a, 2a, and 3a in this figure, recorded at 0.1V/s in anodic scans, present irreversible peaks (this irreversible behaviour was revealed also at the higher scan rate of 1V/s). Moreover, in cathodic scans the 3 processes are irreversible as well. After scanning the first cathodic peak (1c), a new oxidation peak appears (1c') in the reverse sweep. It is shifted with about 1V with respect to 1c, and its current value is much smaller than that for 1c. This behaviour indicates that 1c is an EC process. Both 2c and 3c do not exhibit any response when scanning back to the starting potential. The reduction peak 3c is larger and higher in intensity than 1c, and could imply a multi electron transfer. Peak 2c is overlapped on 3c in the CV scans.

Linear dependences of the peak currents on concentration have been obtained from CV experiments at different concentrations of **1** (inset of fig. 3). Both linear dependences of the peak currents on concentration obtained in DPV and CV (figs. 2, 3) could be used in analytical determinations of **1** by these electrochemical methods.

The reversibility of the first anodic and cathodic processes has been evaluated from the CV curves obtained at different scan rates. Linear dependences of the peak currents on the square root of the scan rate have been obtained (fig. 5, inset). Slopes of about 108 and 135 μA(V/s)$^{-1/2}$ for the peaks 1a, and 1c, respectively, have been obtained in 1mM solution of compound **1**. Both 1a and 1c peaks are not reversible in the range of investigated scan rates.

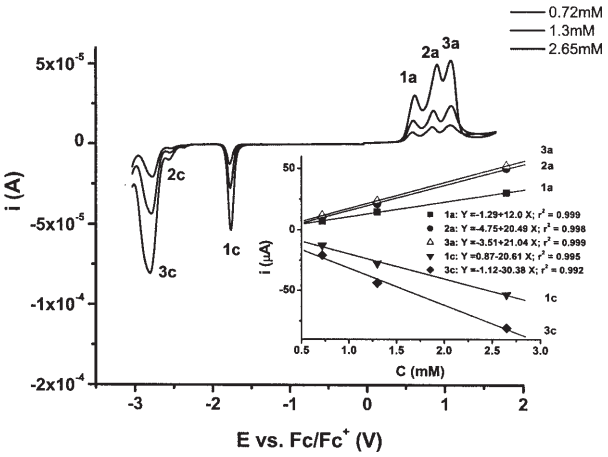

Fig. 2. DPV curves for **1** at different concentrations (mM) on glassy carbon electrode (3mm in diameter) in 0.1M TBAP, CH_3CN. Inset: Dependences of the peak currents (μA) on concentration (mM) of **1**

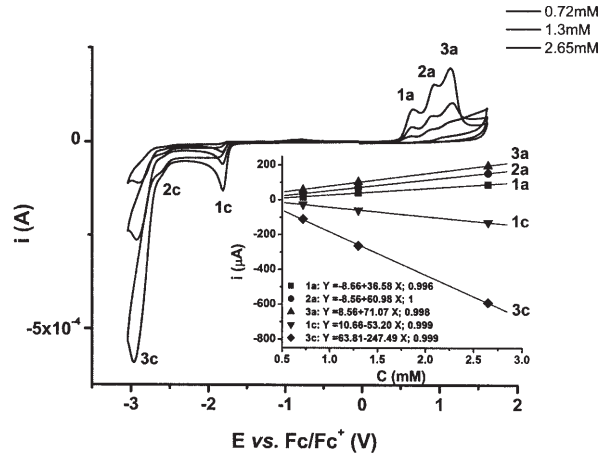

Fig. 3. CV (0.1 V/s) curves for **1** at different concentrations (mM) on glassy carbon electrode (3mm in diameter) in 0.1M TBAP, CH_3CN. Inset: Dependences of the peak currents (μA) on concentration (mM) of **1**

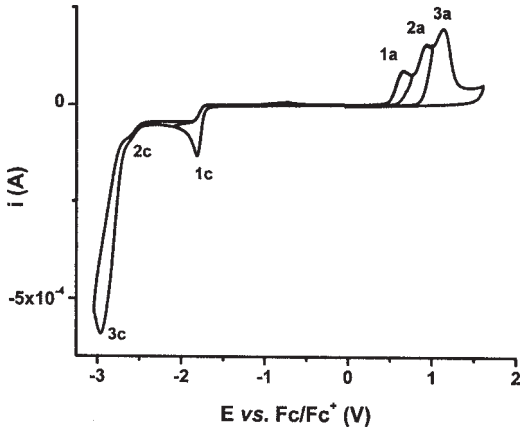

Fig. 4. CV (0.1 V/s) curves for **1** (2.7 mM) at different scan ranges on glassy carbon electrode (3mm in diameter) in 0.1M TBAP, CH_3CN.

The results obtained by DPV and CV were concordant, with respect to peak potentials, and were complementary, yielding specific features for each compound. DPV has enabled the precise determination of oxidation and reduction potentials of characteristic processes leading to unique fingerprints for each compound. The proportionality of the peak current to substrate concentrations has been proved to be a useful test of the analytic value for the DPV

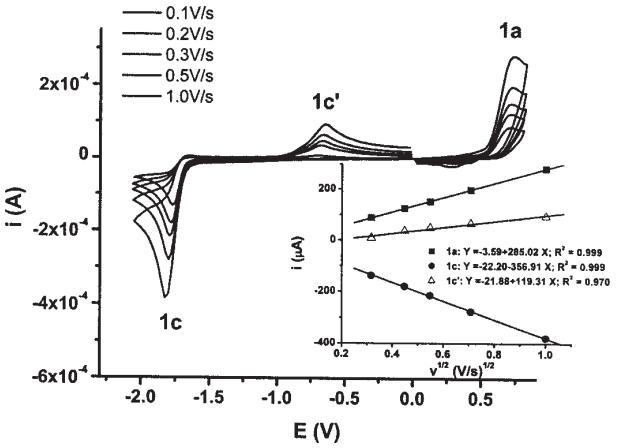

Fig. 5. Influence of the scan rate (υ) on the CV currents on glassy carbon (3mm in diameter) for **1** (2.7mM) in 0.1M TBAP, CH_3CN. Inset: Dependences of the peak currents (in μA) on the square root of the scan rate: 0.1 V/s; 0.2; 0.3; 0.5; 1 V/s

method, while CV allowed establishing the reversible feature of each electrode process.

Comparison between substrates

Similar studies as those presented for compound **1** in figures 2-5 have been performed for each investigated azulene-pyridine, and the results are summarized in tables 1-3. Table 1 shows the DPV and CV potentials of the main peaks for all investigated compounds. The character of the main CV peaks (reversible, quasireversible or irreversible) is also shown in table 1. The equations of linear dependences of the peak currents on concentration are given in table 2 for all compounds. They can be exploited in analytical determinations of these compounds by DPV or CV.

The first oxidation peak noted 1a in the CV and DPV curves of azulenes derivatives is the result of many several successive steps. First of them implies the radical cation generation at the azulene moiety, because the azulene is the structural unit by far the most susceptible to oxidation. The positive charge is probably delocalized mainly on the azulene moiety. The results obtained from CV and DPV curves for the azulene compounds have been correlated to their structure. This assumption is based on the irreversibility of the first oxidation peak corresponding to the formation of a radical cation, which is specific to most azulene derivatives [8]. The generated radical cation could be further stabilized by dimerization because the concentration of the electronic spin at C3 is high. The 3,3'-dimer, resulted after hydrogen elimination, can be further oxidized to the corresponding monocation or dication (scheme 1). The analysis of 1a peak potentials in **1**, **1t** and **1g** is consistent with this scheme. It is known that the 4,6,8-trimethylazulene moiety is more stable due to its symmetrical structure and to the steric protection given by the methyl group. Therefore, in the case where it is present, the generation of dimer occurs slower and the first oxidation step becomes quasireversible, in agreement with the characteristics quasireversible (q) for 1a peak, as shown in table 2 for the compound **1t**. The radical cations formed from the dimer are also more reluctant to interact with the solvent to generate polymers. Therefore, higher oxidation steps become also quasireversible. The peaks 2a, 3a are quasireversible (q), as are presented in table 2. A single clear oxidation potential was observed for guaiazulene group (compounds **1g** and **2g**), because this moiety cannot form dimers due to the presence of a methyl group in position 3 (fig. 6). However, the guaiazulene radical cation could couple to the position 2 of thiophene moiety belonging to another molecule, with generation of an asymmetric dimer. That fact could explain the second oxidation potential for these compounds (fig. 6).

The first peak in reduction (1c) corresponds to the formation of a radical anion, step followed by protonation (scheme 2). The peaks 2c and 3c correspond to multielectron transfer processes connected to the reduction of the azulene moiety, with the formation of the polyenic structures.

The oxidation potential values from table 1 are in agreement with the substituent electronic effects. For the first anodic peak 1a, they are ordered as follows: E**1g**< E**1t**< E**1** and E**2g**< E**2t**< E**2**. These differences are mainly due to the electronic effects of the substituents on the azulene electron density. Thus, the electron releasing capacity exerted by alkyl substituents at trimethyl-azulene (in compounds **1t**, **2t**), as well as by those connected to

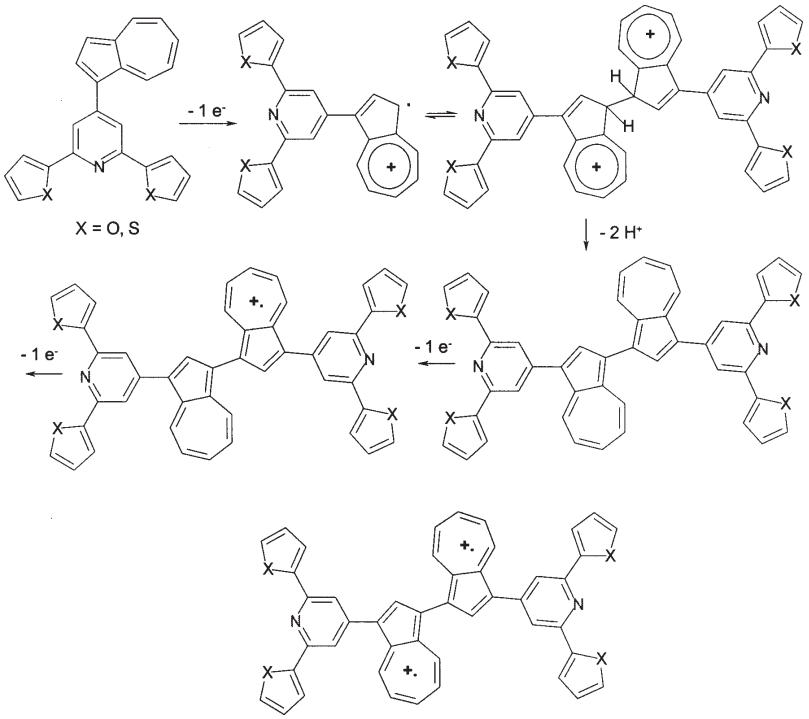

Scheme 1

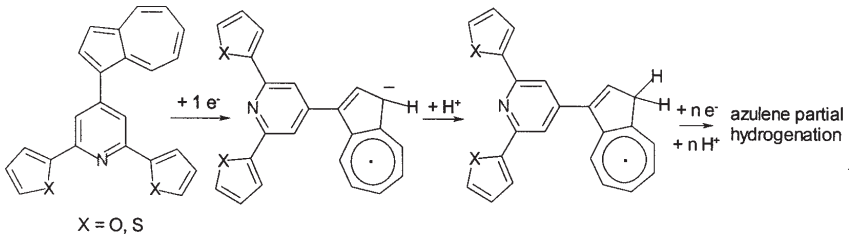

Scheme 2

Table 1
DPV AND CV PEAK POTENTIALS FOR THE COMPOUNDS **1, 1t, 1g, 2, 2t, 2g** (1mM in 0.1M TBAP, CH_3CN) AND ESTIMATION OF REVERSIBILITY BY CV (i = IRREVERSIBLE PEAK; q = QUASIREVERSIBLE PEAK AND r=REVERSIBLE PEAK)

Cpd.	Y	R	-HOMO (eV)	-LUMO (eV)	Method	Peak potential (V)				
						1a	2a	3a	1c	3c
1	O	H	1.2	8.15	*DPV*	*0.595*	*0.856*	*1.076*	*-1.76*	*-2.79*
					CV	0.644i	0.903i	1.16i	-1.82i	-2.93i
1t	O	4,6,8-Me_3	1.09	8.07	*DPV*	*0.52*	*0.67*	*1.26*	*-2.03*	
					CV	0.576q	0.817q	1.398q	-2.08r	
1g	O	8-Me-5iPr	1	7.99	*DPV*	*0.413*			*-1.952*	*-2.85*
					CV	0.456i			-2.02r	-2.96i
2[13]	S	H	1.15	8.09	*DPV*	*0.54*	*0.92*	*1.08*	*-1.82*	*-2.86*
					CV	0.60i	0.94i	1.18i	-1.87i	-2.96i
2t	S	4,6,8-Me_3	1.03	7.95	*DPV*	*0.498*	*0.72*	*1.18*	*-2.06*	*-2.807*
					CV	0.545q	0.776i	1.225i	-2.11r	-2.88i
2g	S	8-Me-5iPr	0.94	7.92	*DPV*	*0.367*		*1.20*	*-2.01*	*-2.827*
					CV	0.41i		1.25i	-2.065r	-2.92i

the guaiazulene moiety (in compounds **1g**, **2g**), increases the electron density on azulene and, therefore, the oxidation potentials of compounds **1g**, **1t** and **2g**, **2t** are lower than those of the pattern compounds **1** and **2**.

In reduction step, the substituent influence on the peak potentials is more complex and, therefore, the first reduction potential was more difficult to be correlated with the substituent. The order is the following in absolute values: E**2t**< E**1t**< E**2g**< E**1g**< E**2**< E**1**. The peak potentials are invariant with concentration both in CV (at the same scan rate), and DPV.

Table 2 presents the equations of the DPV and CV peak currents on substrate concentration for the studied compounds. For all compounds it can be seen that the variations of the anodic peak current with concentration for 1a in the DPV curves have positive slopes of about 10μA/mM, while those obtained from the CV curves have slopes of about 15μA/mM. From analytical point of view, the DPV bigger slopes give more sensitive responses than the CV ones. However, the DPV method allows the identification of these compounds in concentrations much lower than through CV. The variation with concentration of the DPV peak currents for the cathodic peak 1c shows bigger slopes (in absolute value) than those for the anodic peak 1a. This difference could be assessed to a different number of electrons implied in each process.

The influence of the scan rate on CV curves for all compounds is shown in table 3 for the first anodic and cathodic peaks. The comparison of the equations shows mean slopes of about 85 and -105 μA $(V/s)^{-1/2}(mM)^{-1}$ for 1a and 1c, respectively.

The structure of the studied compounds presents a substituted azulene moiety connected (in position 4) to 2,6-bis(2-furyl)- or 2,6-bis(2-thienyl)-pyridine. The alkyls substituents on azulene are all electron releasing substituents. Figure 6 allows a detailed comparison between their DPV curves. The compared peaks are noted for each compound in sequence of their apparition in oxidation (1a, 2a, 3a) or reduction (1c, 2c, 3c) scans. When examining the DPV curves for **1** and **2** (fig. 6), it could be seen that 1a process appears in the DPV of **1** at less negative potential (0.595V) than in **2** (0.54V), while 1c process appears at -1.76V and -1.82V, respectively. The values are in agreement with the electronegativity of the heteroatom in these structures (O is more electronegative than S).

Figure 7 shows the correlation between the experimental oxidation potentials (from DPV and CV) and the highest occupied molecular orbital (HOMO) energies (ionization potentials), computed using the MOPAC program. A good correlation has been obtained from both curves. The evaluation of the reduction potentials shows that it is governed by the same rules as oxidation, but the correlation with the lowest unoccupied molecular orbital (LUMO) energies calculated by MOPAC, given in figure 8, is worse. This could be explained by the fact that the MOPAC program is not sufficiently adequate to correctly

Cpd.	Meth.	Peak				
		1a	2a	3a	1c	2c
1	DPV	Y =-1.29+12.0 X; R^2 = 0.999	Y =-4.75+20.49 X; R^2 = 0.998	Y =-3.51+21.04 X; R^2 = 0.999	Y =0.87-20.61 X; R^2 = 0.995	Y =-1.12-30.38 X; R^2 = 0.992
	CV	Y =-8.66+36.58 X; R^2 = 0.996	Y =-8.56+60.98 X; R^2 = 1	Y =8.56+71.07 X; R^2 = 0.998	Y =10.66-53.2 X; R^2 = 0.999	Y =63.81-247.49 X; R^2 = 0.999
1t	DPV	Y =-1.16+8.29 X; R^2 = 0.998	Y =1.15+5.31 X; R^2 = 0.999	Y =3.8+7.14 X; R^2 = 0.95	Y =2.45-14.27 X; R^2 = 1	
	CV	Y =-1+18.51 X; R^2 = 0.999	Y =-0.79+27.48 X; R^2 = 0.999	Y =12.66+67.68 X; R^2 = 0.997	Y =2.63-21.28 X; R^2 = 0.999	
1g	DPV	Y =0.12+10.99 X; R^2 = 0.999			Y =0.55-14.49 X; R^2 = 0.999	Y =-1.02-17.76 X; R^2 = 0.998
	CV	Y =-1.26+24.25 X; R^2 = 0.999			Y =-5.33-32.13 X; R^2 = 0.999	Y =-2.49-129.34 X; R^2 = 0.999
2 [13]	DPV	Y =2.60+3.07 X; R^2 = 0.880	Y =-0.28+10.95 X; R^2 = 0.987	Y =18.88+8.63 X; R^2 = 0.898	Y =-3.66-8.47 X; R^2 = 0.988	Y =-18.34-16.29 X; R^2 = 0.933
	CV	Y =5.85+11.54 X; R^2 = 0.970	Y =-3.89+38.01 X; R^2 = 0.998	Y =55.02+69.2 X; R^2 = 0.991	Y =-3.45-23.07 X; R^2 = 0.999	Y =-14.72-148.3 X; R^2 = 0.998
2t	DPV	Y =0.51+15.3 X; R^2 = 0.999	Y =1.81+8.15 X; R^2 = 0.999	Y =21.34+17.1 X; R^2 = 0.987	Y =-3.53-21.62 X; R^2 = 0.999	Y =-12.67-46.37 X; R^2 = 0.998
	CV	Y =-2.55+39.52 X; R^2 = 0.999	Y =1.73+49.56 X; R^2 = 0.999	Y =88.9+53.74 X; R^2 = 0.967	Y =-17.56-41.1 X; R^2 = 0.977	Y =-1.65-261.7 X; R^2 = 0.999
2g	DPV	Y =0.715+10.02 X; R^2 = 0.999		Y =11.37+6.85 X; R^2 = 0.979	Y =-1.33-12.13 X; R^2 = 0.998	Y =-11.99-20.5 X; R^2 = 0.999
	CV	Y =0.95+21.14 X; R^2 = 0.999		Y =43+24.61 X; R^2 = 0.999	Y =-8.53-21.85 X; R^2 = 0.972	Y =-9.99-130.79 X; R^2 = 0.996

Table 2
EQUATIONS OF THE DPV AND CV (0.1 V/s) PEAK CURRENTS (*i* in μA) DEPENDENCES ON THE SUBSTRATE CONCENTRATION (*C* IN mM) FOR THE COMPOUNDS **1, 1t, 1g, 2, 2t, 2g** (IN 0.1M TBAP, CH_3CN)

Compound\Peak	1a	1c
1	Y = -1.35+107.55 X; R^2 =0.999 (i)	Y = -8.37-134.7 X; R^2 = 0.999 (i)
1t	Y = -2.41+64.75 X; R^2 = 0.999 (q)	Y = 0.555-67.93 X; R^2 = 0.999 (r)
1g	Y = -3.605+85.19 X; R^2 = 0.999 (i)	Y = -2.715-112.53 X; R^2 = 0.997 (r)
2 [13]	Y = - 12.18+98.445 X; R^2 = 0.999 (i)	Y = -5.745-101.895 X; R^2 = 0.999 (i)
2t	Y = 38.57+97.2 X; R^2 = 0.976 (q)	Y = -46.87-138.8 X; R^2 = 0.980 (r)
2g	Y = 21.81+53.47 X; R^2 = 0.973 (i)	Y = -23.965-73.68 X; R^2 = 0.991 (r)

Table 3
EQUATIONS OF THE DEPENDENCE OF 1a AND 1c CV PEAK CURRENTS CORRESPONDING TO A CONCENTRATION OF 1mM, Y in μA/mM, ON THE SQUARE ROOT OF THE SCAN RATE (V/s), X, FOR THE INVESTIGATED COMPOUNDS

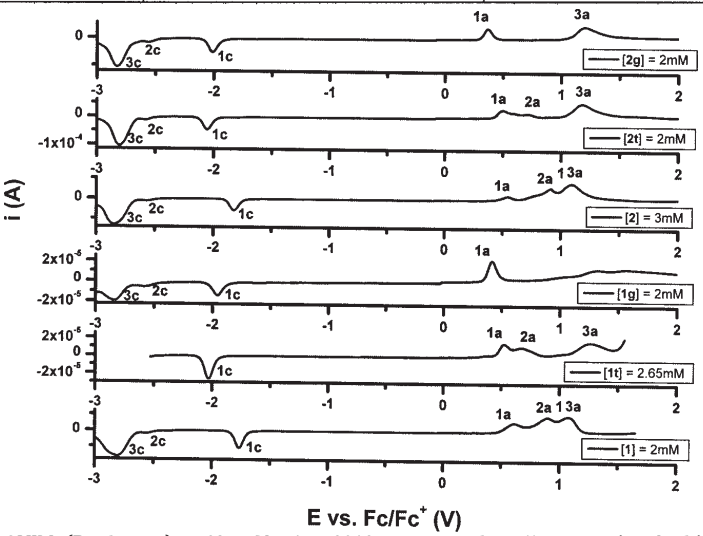

Fig. 6. Anodic and cathodic DPV curves for the investigated compounds in 0.1M TBAP, CH_3CN on glassy carbon (3mm in diameter).

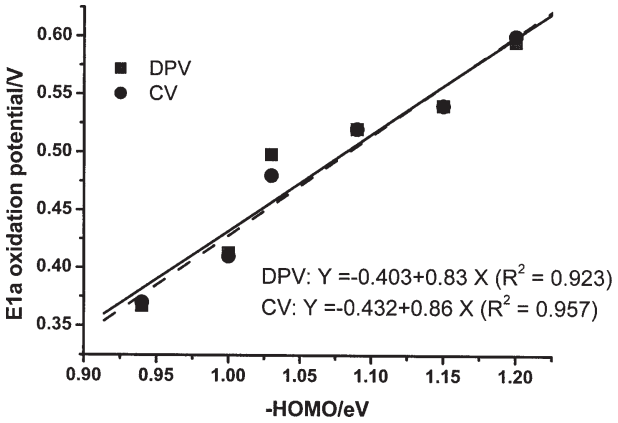

Fig. 7. Correlation between the experimental oxidation potentials *E*1a (from DPV and CV, obtained at concentration of 1mM on glassy carbon, in 0.1M TBAP, CH_3CN) and *E*(HOMO) using AM1 method

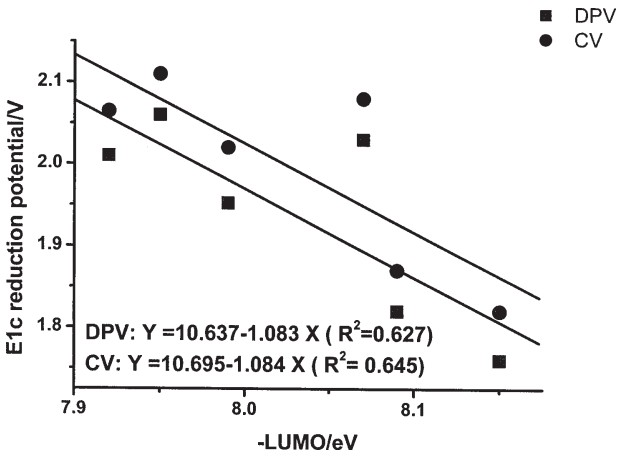

Fig. 8. Correlation between the experimental reduction potentials *E*1c (from DPV and CV, obtained at concentration of 1mM, on glassy carbon in 0.1M TBAP, CH_3CN) and *E* (LUMO) using AM1 method

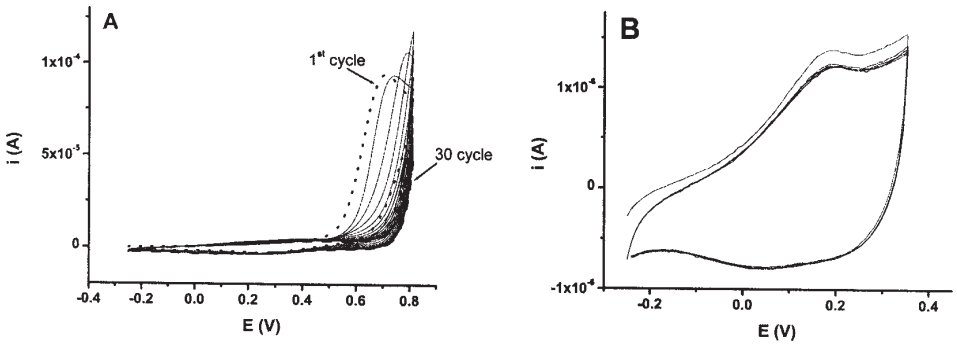

Fig. 9. (A) Successive CV anodic scans on glassy carbon in 2.65mM solution of **1** in 0.1M TBAP, CH_3CN at 0.1 V/s and (B) the CV curves for the modified electrode obtained by CPE (2mC) at 0.805V in transfer solution (0.1M TBAP, CH_3CN at 0.1 V/s).

anticipate the destabilization of the azulene system by an asymmetric substitution.

Film formation

The formation of the polyazulene film has been tried by successive scans in the domains of the first anodic (1a) or first cathodic (1c) processes in millimolar solutions of each compound, in CH_3CN + 0.1 M TBAP. The anodic and cathodic successive curves are given, for instance, for the compound **1** in figure 9. The tendency to polymerize is characteristic only for the unsubstituted 4-(azulen-1-yl)-2,6-bis(2-furyl)pyridine. Conductive polymeric films have been formed on the electrode surface. In successive anodic scans, the oxidation peak is shifted progressively to positive values, indicating the electrode coverage with oxidation products. In repeated cathodic scans, the successive curves were practically unchanged. The films can be grown also by controlled potential electrolysis (CPE) in the same synthesis solution. After the transfer in blank solution (0.1M TBAP, CH_3CN), the obtained modified electrode shows a stable behaviour in CV. Figure 9B presents the CVs recorded during 10 redox cycles. The modified electrode has a couple of peaks which correspond to the oxidation/reduction of the polymeric film.

Conclusions

This work explored the electrochemical properties of several 4-(azulen-1-yl)-2,6-bis(furyl)- and 4-(azulen-1-yl)-2,6-bis(tienyl)-pyridine and established rules concerning the influence of releasing substituents upon their electrochemical behavior. The oxidations were irreversible for the unsubstituted azulene derivatives and for the azulenes substituted with 3,8-Me_2-5-iPr groups, while the azulene substituted with 4,6,8-Me_3 groups has shown quasireversible oxidations. In what concern the reductions, they were irreversible for unsubstituted azulenes, and reversible for the substituted azulenes.

Very good correlations between the experimental oxidation potentials and MOPAC computed ionization potential were found, whereas the correlation of the reduction processes with LUMO energies was poorer. A detailed comparison between their DPV curves shows that both electronic effect of the substituent and heteroatom electronegativity influence the oxidation and reduction potentials. The tendency to polymerize is present only for the unsubstituted 4-(azulen-1-yl)-2,6-bis(2-furyl)pyridine. These films are adherent and have potential applications in cation recognition. The work is in progress.

Acknowledgements: The authors are grateful to European Social Fund through POSDRU/89/1.5/S/54785 project: "Postdoctoral Program for Advanced Research in the field of nanomaterials for financial support.

References

1. LIU X-J, LENG W-N, FENG J-K, REN A-M, Zhou X 2003 Chin. J. Chem. **21(8)** 2015
2. ITO S, KUBO T, MORITA N, IKOMA T, TERO-KUBOTA S, KAWAKAMI J, TAJIRI A., 2005 J. Org. Chem. **70** 2285
3. WALTMAN R J., Bargon J 1986 Can. J. Chem. **64** 76
4. NAOI K, UEYAMA K, OSAKA T 1989 J. Electroanal. Chem. **136** 2444

5. (a) WANG F, LAI Y-H, Han M-Y 2004 Macromolecules **37(9)** 3222; (b) CASADO J, ORTIZ R P, Navarrete J T L 2004 J. Phys. Chem. B **108(48)** 18463; (c) NOLL G, LAMBERT C, LYNCH M, PORSCH M, Daub J 2008 J. Phys. Chem. C **112(6)** 2156; (d) UNGUREANU E-M, AMARANDEI C A, CAVAL D I, BUICA G-O, RAZUS A C, BIRZAN L 2010 Journal of Optoelectronics and Advanced Materials **12(8)** 1805.
6. LASH T D, COLBY D A, GRAHAM SH R, FERRENCE G M, SZCZPURA L F 2003 Inorg. Chem. **42(22)** 7326
7. STEPHAN FRANCIS DEPLAZES in Ph. D. dissertation "Ligand design, coordination and electrochemistry of nonbenzenoid aryl isocyanides", University of Kansas, http://kuscholarworks.ku.edu/dspace/ bitstream/1808/3973/1/umi-ku-2180_1.pdf
8. UNGUREANU E-M, RAZUS A C, BARZAN L, CRETU M-S, BUICA G-O 2008 Electrochim. Acta **53** 7089
9. UNGUREANU E-M, RAZUS A C, BARZAN L, BUICA G-O, CRETU M-S 2005 Univ. Politehnica Bucharest Scient. Bull. **65** 3
10. UNGUREANU E-M, RAZUS A C, BARZAN L, BUICA G-O, CRETU M-S 2005 Univ. Politehnica Bucharest Scient. Bull. **67** 82
11. UNGUREANU E-M, BUICA G-O, RAZUS A C, BIRZAN L, Giol E D 2011 Monatsh. Chem. **142** 243
12. RAZUS A C, BIRZAN L, CRISTEA M, TECUCEANU V, HANGANU A, ENACHE C 2011 J. Heterocycl. Chem. DOI: 10.1002/jhet.684
13. BUICA G-O, UNGUREANU E-M, RAZUS A C, BIRZAN L, BUJDUVEANU M-R, 2011 Electrochim. Acta **56** 5028-5036

Manuscript recieved: 20.06.2011